

ATOMIC CARBON IN SOUTHERN HEMISPHERE HIGH-LATITUDE CLOUDS

JAMES G. INGALLS, RICHARD A. CHAMBERLIN,¹ T. M. BANIA, AND JAMES M. JACKSON

Department of Astronomy, Boston University, 725 Commonwealth Avenue, Boston MA 02215;
ingalls@bu.edu, cham@ulu.submm.caltech.edu, bania@bu.edu, jackson@bu.edu

AND

ADAIR P. LANE AND ANTONY A. STARK

Smithsonian Astrophysical Observatory, 60 Garden Street, Mail Stop 78, Cambridge MA 02138;
adair@cfa.harvard.edu, aas@cfa.harvard.edu

Received 1996 August 23; accepted 1996 November 4

ABSTRACT

We report the detection of atomic carbon in a sample of eight southern hemisphere high Galactic latitude molecular clouds, using the Antarctic Submillimeter Telescope and Remote Observatory. The 492 GHz ($^3P_1 \rightarrow ^3P_0$) transition of [C I] was detected in all of the clouds observed. The C/CO column density ratio ranges from 0.4 to 2.5 and is similar to the values previously measured in high-latitude clouds MBM 12 and HD 210121. For all 10 high-latitude clouds observed in [C I], C/CO averages ~ 1.2 and decreases with increasing total gas column density N_{H} , as predicted by translucent cloud models. Quantitative comparison with chemical models of homogeneous clouds is unsatisfactory, however, and we conclude that the clumpy structure of clouds must be taken into account in order to interpret the data properly.

Subject headings: ISM: abundances — ISM: atoms — ISM: clouds — ISM: molecules — infrared: ISM: lines and bands

1. INTRODUCTION

The high Galactic latitude ($b \gtrsim 15^\circ$) molecular clouds (HLCs; see Magnani, Hartmann, & Speck 1996, and references therein) are an important class of objects the study of which can address many questions about molecule formation in the interstellar medium. The HLCs are predominantly translucent clouds ($A_v \approx 1\text{--}5$; van Dishoeck & Black 1988) associated with *IRAS* cirrus (Low et al. 1984). Models of the chemistry in translucent clouds (e.g., van Dishoeck & Black 1988) indicate that they are the transition objects between clouds with most of their carbon in atomic form and most of their carbon in CO. Translucent clouds are thus the simplest regions in which molecules exist in abundance and where photo processes dominate the chemistry.

The high-latitude molecular clouds account for only 10%–20% of the local molecular mass surface density (Magnani et al. 1996). However, large-scale surveys imply that most of the molecular gas in the Galaxy is translucent. Polk et al. (1988) determined that a significant amount of the ^{12}CO emission in the Galactic plane is produced by molecular gas with a lower opacity than that of giant molecular clouds (GMCs). Furthermore, Chiar et al. (1994) modeled CO ($J = 2\text{--}1$) and ($J = 1\text{--}0$) measurements of the Galactic molecular ring as consisting of $\sim 40\%$ GMCs and $\sim 60\%$ translucent clouds. It is therefore likely that the HLCs sample the average population of molecular gas in the Galaxy.

As an ensemble, the HLCs are the nearest molecular clouds to the Sun ($\langle d \rangle \approx 105$ pc; Magnani et al. 1996). Thus the gas distribution can be mapped at high spatial resolution. In addition, most HLCs are far from sources of far-ultraviolet (FUV) ($6\text{ eV} < h\nu < 13.6\text{ eV}$) radiation, and probably receive FUV fluxes equal to the average local interstellar radiation field ($G_0 \sim 1$, in units of the Habing

flux $\approx 1.6 \times 10^{-3}$ ergs cm^{-2} s^{-1} ; Habing 1968). The simplicity of these clouds makes them particularly amenable to photochemical modeling (van Dishoeck & Black 1988; Hollenbach, Takahashi, & Tielens 1991; Spaans 1996).

The dominant formation mechanism of neutral atomic carbon (C) is the photodissociation of CO. In addition, C is predicted to occur in the regions of clouds where H_2 is the most abundant species but in which CO is undetectable. Thus C may be one of the best tracers of translucent molecular gas. Consequently, our understanding of translucent gas is incomplete without carbon measurements. The lowest lying transition of neutral atomic carbon, the [C I] 492 GHz ($^3P_1 \rightarrow ^3P_0$) fine-structure transition, has thus far been reported in only two HLCs. Ingalls, Bania, & Jackson (1994, hereafter IBJ; 1997) detected C I toward 10 ^{13}CO cores in MBM 12 (Lynds 1457–8), the nearest known molecular cloud ($d \approx 65$ pc). For these cores they measured an average value of the C/CO column density ratio of ~ 0.8 . Stark & van Dishoeck (1994) observed C I in the molecular cloud toward HD 210121; based on modeling, their data for two positions gave C/CO column density ratios ranging from 3–6. Since the C/CO abundance ratio is $\gtrsim 1$, these HLCs indeed sample the transition between atomic and molecular carbon-bearing species.

The recently installed Antarctic Submillimeter Telescope and Remote Observatory (AST/RO) has begun a program to study the photochemistry of translucent HLCs. The exceptionally dry atmosphere above the South Pole allows for measurements of C I in HLCs with unprecedented sensitivity. We present here the first results of the AST/RO survey of the ($^3P_1 \rightarrow ^3P_0$) fine-structure transition of [C I] in eight southern hemisphere high-latitude clouds.

2. OBSERVATIONS

2.1. *The Source Sample*

Eight HLCs at southern declinations listed in the catalog of Keto & Myers (1986) were observed. Source identifica-

¹ Current address: Caltech Submillimeter Observatory, Hilo, HI 96720.

tions and positions are listed in Table 1. The clouds are the objects in the Keto & Myers catalog which fall in the declination range $-25^\circ > \delta > -80^\circ$ (at the South Pole $-\delta$ is elevation). The sample clouds have thus far only been studied in CO at 8.7 angular resolution (Keto & Myers 1986), except for cloud G225.3–66.3, which has also been observed at higher angular resolution in CO and in the photographic *B* band (Stark 1995).

Most of the clouds in our sample are isolated translucent clouds without embedded stars. Two objects are exceptions: G294.4–14.3 is a translucent region located on the fringe of a molecular cloud in the Chamaeleon dark cloud complex, and G316.5+21.0 contains a young star (see § 4.2). Such objects bridge the gap between isolated translucent clouds and star-forming dark clouds.

2.2. Atomic Carbon Observations

Observations of the ($^3P_1 \rightarrow ^3P_0$) transition of [C I] at 492.1607 GHz were made during the 1995 Austral winter with the AST/RO 1.7 m diameter telescope located at the National Science Foundation Amundsen-Scott South Pole Station. AST/RO operates at submillimeter wavelengths and is a flexible, general purpose instrument capable of making a wide variety of spectroscopic measurements for both astronomy and aeronomy (Stark et al. 1994, 1997a). The telescope efficiency at 492 GHz was estimated from skydip measurements (Chamberlin, Lane, & Stark 1997) to be $\eta_l = 0.75$. Measurements of the moon surface brightness suggest that this value is close to the main-beam efficiency η_{MB} . We thus adopt 0.75 for the main-beam efficiency. The beam shape was determined using limb scans of the moon, continuum maps of Jupiter, and spectral line maps of compact sources (Stark et al. 1997a). For the observations reported here, the half-power beamwidth of the telescope at 492 GHz was $\sim 140''$, corresponding to a 14,000 AU spatial resolution at 100 pc.

The carbon line was measured using a quasi-optical SIS receiver (Zmuidzinas & LeDuc 1993; Engargiola, Zmuidzinas, & Lo 1994), which had a 165 K double sideband (DSB) receiver noise temperature. The intermediate frequency output was sampled by a 2048 channel, 1.4 GHz bandwidth acousto-optical spectrometer (AOS) (Schieder, Tolls, & Winnewisser 1989). The velocity resolution was 0.67 km s^{-1} . System noise temperatures ranged between 700 and 1500 K. During the 1995 Austral winter the

median 492 GHz zenith atmospheric opacity for the South Pole site was 0.70 (Chamberlin et al. 1997).

The HLC observations were made on 1995 September 12–14. The [C I] spectra were obtained by position-switching 1° in azimuth, well outside the IRAS 100 μm boundaries of the clouds. Because of the unique geographical location of the telescope, position-switched offsets were both at constant elevation and fixed on the sky.

Intensity calibration was accomplished by measuring blackbody loads at 40 and 90 K, as well as an ambient temperature load (Stark et al. 1997a, 1997b). In order to correct for atmospheric attenuation, skydips were performed at intervals of approximately 6 hr. In addition, measurements of the sky brightness temperature were made at the position of the current source every 10–15 minutes. A slab model of the atmosphere was assumed, and an atmospheric zenith opacity was computed (see Chamberlin et al. 1996) and subsequently used to correct the data for atmospheric attenuation. Finally, the overall intensity calibration was checked by observing the compact H II region G305.3+0.2 once before observing each HLC. This procedure yielded intensities repeatable to $\pm 30\%$. Since the intensity of G305.3+0.2 was a function of azimuth, this error is primarily due to pointing uncertainties of $\sim 30''$ rms (Stark et al. 1997a).

3. RESULTS

3.1. Observed [C I] - Properties of High-Latitude Clouds

The [C I] ($^3P_1 \rightarrow ^3P_0$) transition was detected in all of the clouds we observed. Because this was a preliminary survey based upon the Keto & Myers CO data which had rather coarse angular resolution, the nominal center of each cloud was mapped in a 3×3 pixel fully sampled grid. The spectra were then averaged to form a $\sim 5'$ diameter “superbeam.” For the source maps the total on-source integration times range from 2.5 to 3.5 hr.

The average [C I] spectra are shown in Figure 1 for each source. Linear baselines were subtracted from these spectra. Intensities are main-beam brightness temperatures, T_{MB} , that is, Rayleigh-Jeans antenna temperature T_A corrected for both atmospheric attenuation and main-beam efficiency ($T_{MB} \equiv T_A^*/\eta_{MB}$).

The observed parameters for the [C I] emission from the sample HLCs are summarized in Table 1. A Gaussian profile was fitted to each of the [C I] spectra; these fits are

TABLE 1
OBSERVED PROPERTIES OF SOUTHERN HIGH-LATITUDE CLOUDS

CLOUD ^a	$\alpha(1950.0)^a$	$\delta(1950.0)^a$	C I ($^3P_1 \rightarrow ^3P_0$)			
			V_{LSR}^b (km s^{-1})	ΔV_{FWHM}^b (km s^{-1})	T_{MB}^c (K)	I_{100}^d (MJy ster^{-1})
G225.3–66.3	02 36 45.6	–29 49 01	0.9	2.6 ± 0.2	0.2 ± 0.1	5.4 ± 0.5
G295.3–36.2	03 08 27.3	–79 05 34	2.2	2.0 ± 0.1	0.4 ± 0.1	0.6 ± 0.5
G259.5–16.5	07 12 30.1	–48 25 59	3.8	2.1 ± 0.1	0.3 ± 0.1	10.8 ± 0.5
G292.7–19.8	09 14 08.4	–77 45 13	4.4	2.2 ± 0.1	0.5 ± 0.2	1.8 ± 0.5
G294.6–19.7	09 41 32.8	–79 07 34	5.2	1.9 ± 0.1	0.3 ± 0.1	2.2 ± 0.5
G294.4–14.3 Cha	10 34 04.5	–74 30 05	4.4	2.0 ± 0.0	0.3 ± 0.1	2.9 ± 0.5
G272.9+29.3	10 52 14.3	–26 20 25	–3.5	1.6 ± 0.2	0.3 ± 0.1	4.2 ± 0.5
G316.5+21.0	13 54 43.9	–39 44 53	–6.0	2.2 ± 0.0	1.0 ± 0.3	96.1 ± 0.5

^a Cloud positions taken from Keto & Myers (1986).

^b Determined from a Gaussian fit to the line.

^c Intensity of peak emission. 30% calibration uncertainty assumed.

^d IRAS 100 μm intensity, averaged over a $5'$ diameter circle.

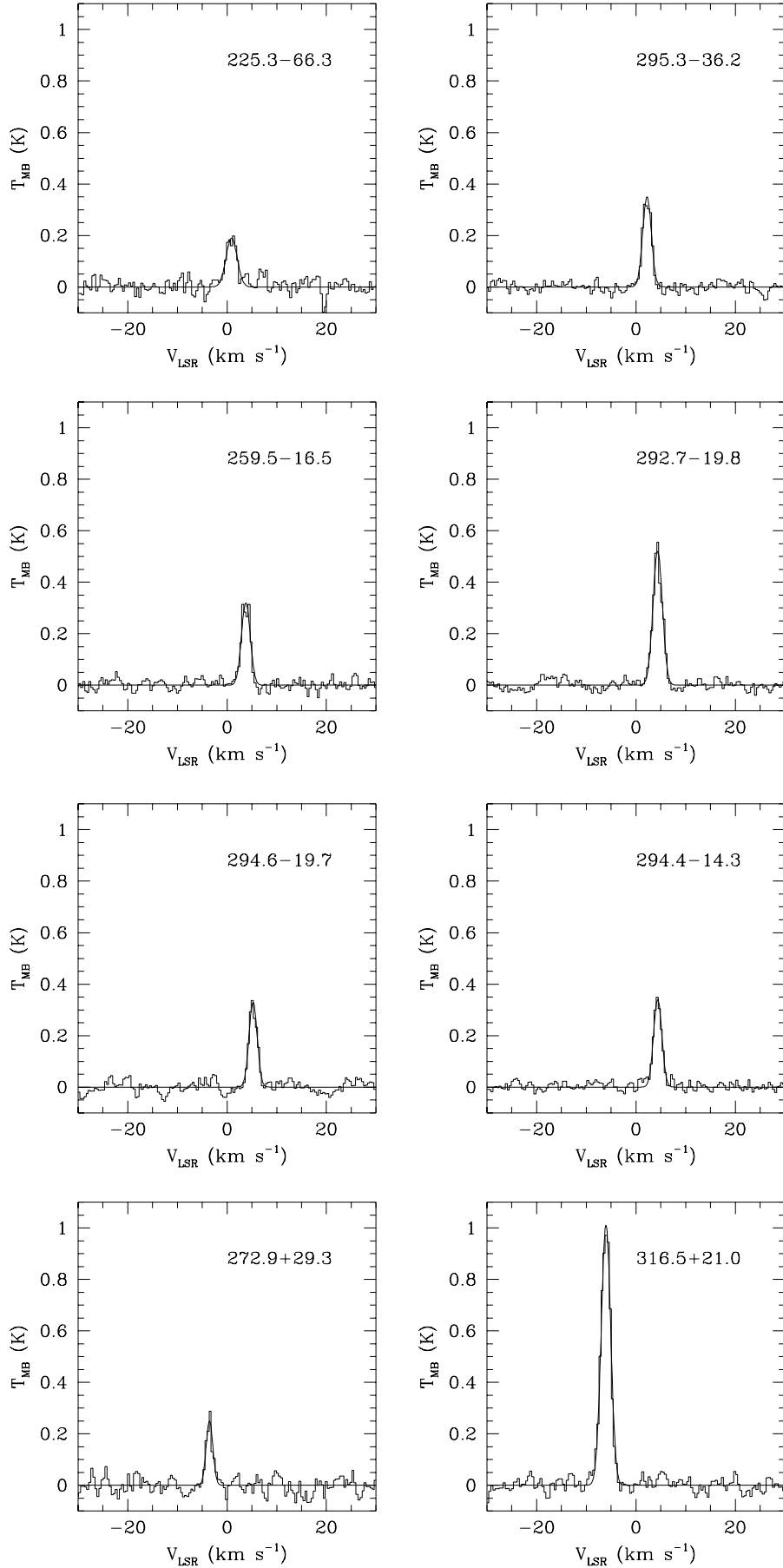


FIG. 1.—[C I] ($^3P_1 \rightarrow ^3P_0$) spectra of eight high-latitude molecular clouds (see Table 1), taken with the AST/RO telescope. The velocity resolution of the spectra is $\delta V = 0.67 \text{ km s}^{-1}$. A linear baseline has been removed from the data. Gaussian fits have been superimposed on the spectra.

superimposed on the spectra in Figure 1. The resulting values for line center, V_{LSR} , line width, ΔV_{FWHM} , and line peak intensity, T_{MB} , are listed in Table 1. The observed [C I] properties of these clouds are consistent with the assertion, based on CO observations, that the HLCs are local, turbulent objects. The average LSR velocity for these HLCs is $\langle V_{\text{LSR}} \rangle = 1.4 \pm 4.1 \text{ km s}^{-1}$, which is consistent with the HLCs being local; the average linewidth is $\langle \Delta V_{\text{FWHM}} \rangle = 2.1 \pm 0.1 \text{ km s}^{-1}$, much greater than the thermal velocity dispersion of $\sim 0.1 \text{ km s}^{-1}$ for 10 K carbon gas, which shows that the clouds are turbulent. The average [C I] intensity is $\langle T_{\text{MB}} \rangle = 0.4 \pm 0.1 \text{ K}$.

Estimates of the [C I] column density in each cloud can be made as follows. We have calculated the [C I] ($^3P_1 \rightarrow ^3P_0$) line center optical depth τ_{10} , by assuming homogeneous clouds in local thermodynamic equilibrium (LTE):

$$\tau_{10} = -\ln \left[1 - \frac{T_{\text{MB}}}{J_\nu(T_{\text{ex}}) - J_\nu(2.7 \text{ K})} \right], \quad (1)$$

where J_ν is the radiation temperature

$$J_\nu(T) \equiv \frac{h\nu_{10}/k}{e^{h\nu_{10}/kT} - 1} \quad (2)$$

and T_{ex} is the excitation temperature. For [C I] ($^3P_1 \rightarrow ^3P_0$), $h\nu_{10}/k = 23.6 \text{ K}$. We estimate the total beam-averaged atomic carbon column densities, N_{C} :

$$N_{\text{C}} = 2.49 \times 10^{16} \tau_{10} \left(\frac{\Delta V_{\text{FWHM}}}{1 \text{ km s}^{-1}} \right) \frac{Z(T_{\text{ex}})}{1 - e^{(-23.6 \text{ K})/T_{\text{ex}}}} \text{ cm}^{-2}, \quad (3)$$

where ΔV_{FWHM} is the Gaussian linewidth and $Z(T_{\text{ex}})$ is the ground state partition function for the carbon atom

$$Z(T_{\text{ex}}) = 1 + 3e^{(-23.6 \text{ K})/T_{\text{ex}}} + 5e^{(-62.5 \text{ K})/T_{\text{ex}}}. \quad (4)$$

We assume an excitation temperature $T_{\text{ex}} \sim 10 \text{ K}$, which is typical for the molecular cores in the MBM 12 cloud (Pound, Bania, & Wilson 1990). The values of τ_{10} and N_{C} derived under these assumptions are listed in Table 2. We list values for the eight southern HLCs observed with AST/RO and cloud averages $\langle \tau_{10} \rangle$ and $\langle N_{\text{C}} \rangle$ for the other

known [C I] sources MBM 12 and HD 210121. The averages for MBM 12 and HD 210121 were estimated using the average measured [C I] line parameters in IBJ and Stark & van Dishoeck (1994), respectively. Note that the atomic carbon column densities quoted in Stark & van Dishoeck (1994) for HD 210121 are the result of statistical equilibrium calculations for a range of cloud densities and temperatures, whereas here we make the LTE assumption with $T_{\text{ex}} = 10 \text{ K}$.

3.2. Total Gas Column Densities in HLCs

All large-scale surveys of neutral atomic hydrogen at high Galactic latitudes have angular resolutions exceeding $11'$, which is far too coarse to be useful in estimating the H I column densities toward our HLC sample objects. We can, however, use the $\sim 3'$ *IRAS* 100 μm images of these regions to estimate total neutral gas column densities N_{H} . Photoelectric absorption of $\frac{3}{4} \text{ keV}$ X-rays by neutral gas (predominantly H, H_2 , and He) associated with the dust responsible for *IRAS* 100 μm emission yields an anticorrelation between the $\frac{3}{4} \text{ keV}$ and 100 μm intensities. This anticorrelation has been measured for the high-latitude cloud MBM 12 by Snowden, McCammon, & Verter (1993). Assuming solar abundances for the cloud, they derived the conversion factor

$$N_{\text{H}}/I_{100} \sim 1.3_{-0.1}^{+1.1} \times 10^{20} \text{ cm}^{-2} (\text{MJy ster}^{-1})^{-1}. \quad (5)$$

This ratio is very close to the ratio of H I column density to 100 μm brightness derived toward high-latitude regions by Boulanger & Péroult (1988). Since those authors avoided lines of sight crossing molecular clouds, most of the gas they studied was probably atomic. In such regions, H I emission traces total gas column density quite well. Thus the results of Snowden et al. (1993) are entirely compatible with those of Boulanger & Péroult (1988). If we assume that equation (5) is valid for all HLCs, *IRAS* 100 μm images can be used to estimate beam-averaged total neutral gas column densities, N_{H} .

We have obtained HIRES-processed 100 μm images of the Table 1 clouds and measured the average value of I_{100} in a $5'$ aperture centered on the nominal position of each cloud. The measured values of I_{100} are listed in Table 1. In some cases, the Keto & Myers (1986) cloud positions were

TABLE 2
DERIVED LTE^a PROPERTIES OF HIGH-LATITUDE CLOUDS

Cloud	τ_{10}	$N_{\text{C}}(10^{16} \text{ cm}^{-2})$	$N_{\text{CO}}(10^{16} \text{ cm}^{-2})$	$N_{\text{H}}^b(10^{20} \text{ cm}^{-2})$	$N_{\text{C}}/N_{\text{CO}}^d$	$N_{\text{C}}/N_{\text{H}}$
G225.3–66.3	0.1 ± 0.0	2.5 ± 1.4	$< 3.0^c$	$7.0_{-0.8}^{+6.0}$	> 0.8	$3.5_{-2.0}^{+3.6} \times 10^{-5}$
G295.3–36.2	0.2 ± 0.1	3.7 ± 1.1	1.5 ± 0.5^c	$0.8_{-0.7}^{+0.9}$	$2.4_{-0.9}^{+1.5}$	$4.7_{-4.2}^{+5.8} \times 10^{-4}$
G259.5–16.5	0.1 ± 0.1	3.4 ± 1.1	7.1 ± 0.6^c	$14.0_{-1.3}^{+11.9}$	$0.5_{-0.2}^{+0.2}$	$2.4_{-0.8}^{+2.2} \times 10^{-5}$
G292.7–19.8	0.2 ± 0.1	6.3 ± 2.7	2.6 ± 0.6^c	$2.3_{-0.7}^{+2.1}$	$2.4_{-1.4}^{+1.3}$	$2.7_{-1.4}^{+2.6} \times 10^{-4}$
G294.6–19.7	0.1 ± 0.1	3.3 ± 1.1	9.2 ± 1.1^c	$2.9_{-0.7}^{+2.5}$	$0.4_{-0.1}^{+0.1}$	$1.1_{-0.5}^{+1.1} \times 10^{-4}$
G294.4–14.3 Cha.....	0.2 ± 0.1	3.4 ± 1.1	$< 3.2^c$	$3.8_{-0.7}^{+3.2}$	> 1.1	$9.1_{-3.4}^{+8.4} \times 10^{-5}$
G272.9+29.3	0.1 ± 0.1	2.0 ± 0.8	$< 2.7^c$	$5.5_{-0.8}^{+4.7}$	> 0.7	$3.7_{-1.6}^{+3.5} \times 10^{-5}$
G316.5+21.0	0.5 ± 0.2	13.1 ± 5.2	19.8 ± 1.5^c	$125.0_{-9.6}^{+105.7}$	$0.7_{-0.3}^{+0.3}$	$1.0_{-0.4}^{+1.0} \times 10^{-5}$
$\langle \text{MBM12} \rangle$	1.5 ± 1.1^e	33.4 ± 2.4^e	37.8 ± 14.4^e	$29.9_{-2.4}^{+25.3}$	$0.8_{-0.2}^{+0.6}$	$1.1_{-0.8}^{+1.2} \times 10^{-4}$
$\langle \text{HD210121} \rangle$	1.0 ± 0.3^f	20.1 ± 6.7^f	16.1 ± 5.9^f	$13.0_{-1.2}^{+11.0}$	$1.2_{-0.5}^{+0.9}$	$1.5_{-0.5}^{+1.4} \times 10^{-4}$

^a $T_{\text{ex}} = 10 \text{ K}$.

^b Total gas column density. Estimated using the I_{100}/N_{H} conversion of Snowden et al. (1993).

^c N_{CO} estimates based on ^{13}CO line parameters in Keto & Myers (1986). Error bars are 30%, upper limits are 3σ .

^d Error bars give the 1σ confidence interval in this ratio.

^e MBM 12 data for C and CO are the average over ten positions (Ingalls et al. 1996; IBJ).

^f HD 210121 data for C and CO are based on line parameters in Stark & van Dishoeck (1994).

found to be far from the peak of I_{100} . Conservative standard errors of $0.5 \text{ MJy ster}^{-1}$ were assumed for the *IRAS* measurements. In Table 2 we list N_{H} and the fractional abundance of atomic carbon, $N_{\text{C}}/N_{\text{H}}$, for all HLCs observed in [C I] to date.

3.3. The C/CO Column Density Ratio in HLCs

We can estimate the C/CO column density ratio in the sample clouds from ^{13}CO measurements (Keto & Myers 1986) made toward the Table 1 positions. Although the angular resolutions of the ^{13}CO and [C I] observations are different (8.7 for ^{13}CO , $\sim 5'$ for [C I]), a preliminary C/CO ratio can be derived. The C/CO ratio can in fact be underestimated by no worse than a factor of 3 because of beam sampling effects. Keto & Myers (1986) assumed optically thick ^{12}CO lines and LTE to derive excitation temperatures for the clouds with detectable ^{13}CO lines. The derived values of T_{ex} for the Table 1 sources range from 6 to 11 K. For comparison with the [C I] data, we assume $T_{\text{ex}} = 10$ K. We have derived $N(^{13}\text{CO})$ from the line measurements of Keto & Myers (1986). Assuming an abundance ratio $[^{12}\text{CO}]/[^{13}\text{CO}] \approx [^{12}\text{C}]/[^{13}\text{C}] = 62$ (Langer & Penzias 1993), we estimate the column density of ^{12}CO and the resulting column density ratio C/CO. We list N_{CO} and $N_{\text{C}}/N_{\text{CO}}$ in Table 2. For the three clouds not detected in ^{13}CO , we give 3σ upper limits for N_{CO} . In addition, we computed LTE cloud averages, $\langle N_{\text{CO}} \rangle$ and $\langle \text{C/CO} \rangle$, for MBM 12 and HD 210121 using ^{13}CO line parameters compiled by IBJ and Stark & van Dishoeck (1994), respectively.

4. DISCUSSION

4.1. Implications for Photochemical Modeling

These new observations have substantially increased the number of HLCs with measured atomic carbon abundances. Here we make a preliminary comparison of the atomic and molecular gas properties of the HLCs. In Figure 2 we plot the C/CO column density ratio versus N_{H} . Total gas column densities for the nine non-star-forming HLCs (see § 4.2) span the range $N_{\text{H}} = (0.8\text{--}30) \times 10^{20} \text{ cm}^{-2}$. Equivalently, visual extinctions are $A_v = 0.08\text{--}3.0 \text{ mag}$ [since $A_v(\text{mag}) \approx 10^{-21} N_{\text{H}}$]. The C/CO column density ratio in these objects ranges from 0.4 to 2.5 and varies inversely with total gas column density, N_{H} .

For comparison, we show in Figure 2 the results of a chemical equilibrium calculation for four homogeneous translucent clouds with total gas volume density $n_{\text{H}} = 5 \times 10^5, 5 \times 10^4, 5000, \text{ and } 400 \text{ cm}^{-3}$. These models span the range of likely densities of high-latitude molecular gas, from the diffuse envelopes of clouds, where $n_{\text{H}} \sim 100\text{--}500 \text{ cm}^{-3}$ (Gir, Blitz, & Magnani 1994; Minh et al. 1996), to the CO-emitting regions where $\langle n_{\text{H}} \rangle \sim 1000 \text{ cm}^{-3}$ (van Dishoeck et al. 1991), to the dense cores where $n_{\text{H}} \sim 10^4\text{--}10^5 \text{ cm}^{-3}$ (Reach et al. 1995). The model clouds have a kinetic temperature $T_k = 10$ K and an FUV radiation field of intensity $G_0 = 1$ incident on one edge. The model calculates the depth-dependent equilibrium abundances of 27 chemical species containing H, He, C, and O, which undergo a network of 134 gas phase reactions. The total abundance of each element is constrained to its solar value (Anders & Grevesse 1989). Self-shielding of H_2 and CO and shielding of CO by H_2 are taken into account in the calculations (Tielens & Hollenbach 1985; van Dishoeck & Black 1988).

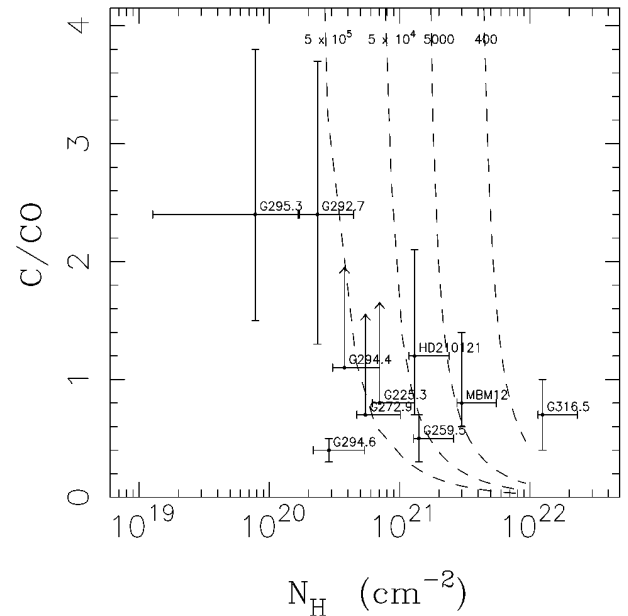


FIG. 2.—Comparison of the C/CO column density ratio with total gas column density N_{H} for translucent clouds. The observed values of C/CO vs. N_{H} for the 10 high-latitude clouds observed in [C I] are plotted as dots with error bars. Lower limits are represented by upward-pointing arrows. The dashed curves are the results of chemical model calculations for homogeneous translucent clouds with $T_k = 10$ K, $G_0 = 1$, and total gas volume densities $n_{\text{H}} = 5 \times 10^5, 5 \times 10^4, 5000, \text{ and } 400 \text{ cm}^{-3}$.

The resulting depth-dependent volume densities for each chemical species are integrated to obtain column densities. The curves in Figure 2 are the resulting values of $N_{\text{C}}/N_{\text{CO}}$ versus total gas column density $N_{\text{H}} \approx N(\text{H}) + 2N(\text{H}_2)$ for the four model clouds.

Qualitatively, the observed trend is reproduced by translucent cloud models (Fig. 2; cf. the more sophisticated models of van Dishoeck & Black 1988; Hollenbach et al. 1991; and Spaans 1996). The models predict translucent clouds to be the transition objects between clouds with most of their carbon as C and clouds with most of their carbon as CO. The average observed value of the C/CO ratio, $\langle \text{C/CO} \rangle \sim 1.2$, confirms this prediction. The detection of significant amounts of atomic carbon in low-extinction molecular regions has important consequences for the study of translucent gas in the Galaxy. In these low- A_v regions, [C I] is just as effective a tracer of molecular gas as CO. In fact, there should exist a population of translucent molecular clouds with low enough A_v that CO is undetectable ($N_{\text{CO}} \lesssim 10^{15} \text{ cm}^{-2}$), and thus in which [C I] is a *better* tracer of H_2 than CO.

Quantitatively, the C/CO versus N_{H} data are not well explained by homogeneous cloud models. The homogeneous models imply inordinately high gas volume densities ($n_{\text{H}} \gtrsim 10^6 \text{ cm}^{-3}$) in regions the size of the AST/RO beam ($\sim 30,000$ AU) in the low- N_{H} clouds. It is possible to compare beam-averaged observations of clumps to the homogeneous models, provided the clumps themselves are homogeneous. A beam-averaged measurement of, e.g., N_{H} is decreased from the actual value in the emitting clumps by the surface filling factor, $N_{\text{H,observed}} \sim \phi N_{\text{H,clump}}$. Assuming that the [C I] ($^3P_1 \rightarrow ^3P_0$), ^{13}CO ($J = 1\text{--}0$), and *IRAS* 100 μm emission arise from the same clumps and that the clumps are uniformly distributed, observations of each of these tracers will have similar values of ϕ . Consequently, the

effects of beam dilution are mitigated somewhat by taking a ratio of two beam-averaged measurements,

$$\frac{N_{\text{C,observed}}}{N_{\text{CO,observed}}} \sim \frac{N_{\text{C,clump}}}{N_{\text{CO,clump}}}. \quad (6)$$

The main difficulty with the interpretation of Figure 2 is thus scaling N_{H} by the appropriate values for ϕ .

Heithausen (1996) has asserted that the volume filling factor of molecular gas in high-latitude clouds is less than 1%, i.e., the surface filling factor is $\phi \lesssim 5\%$ (since $\phi \propto \phi_{\text{volume}}^{2/3}$). Taking this value for ϕ , our C/CO versus N_{H} measurements are consistent with the model predictions for homogeneous clumps with volume densities $n_{\text{H}} \sim 10^3\text{--}10^5 \text{ cm}^{-3}$. The existence of dense gas in high-latitude clouds has been observationally verified: Reach et al. (1995) surveyed seven HLCs, including MBM 12, in the dense gas tracers CS, HCO⁺, and HCN. They detected all three tracers in MBM 12 and found that the CS emission was subthermally excited, indicating densities $n_{\text{H}} \sim 10^4\text{--}10^5 \text{ cm}^{-3}$. Their modeling of the dense cores in cloud MBM 7 indicates that the CS-emitting clumps in the cloud are a factor of ~ 10 smaller in linear size than the CO-emitting clumps in which they are embedded (cf., Turner 1993), so indeed $\phi \ll 1$ for the dense gas.

While our observations and LTE analysis have confirmed the overall trend predicted by photochemical models of translucent clouds, a more general exploration of the parameter space in the chemical models, including a clumpy medium (e.g., Spaans 1996), coupled with statistical equilibrium calculations and more realistic radiative transfer of the C and CO line intensities, is required to interpret the data properly.

4.2. The Star-Forming HLC G316.5 + 21.0

Most HLCs are probably not gravitationally bound but are confined by the ambient ISM pressure (Keto & Myers 1986). Their star-forming efficiency is unknown (e.g., see Magnani et al. 1995). In dark clouds (clouds with $A_v \gtrsim 5$ mag) which often have ongoing low-mass star formation, the interstellar FUV radiation field does not penetrate to their cores. Star formation is thus most affected by the density and mass distribution of the gas. For translucent clouds, however, the FUV opacity of the gas and dust, as well as the confining pressure of the interstellar medium, must also come into play. The most often-studied HLC with ongoing star formation is MBM 12. There are at least two T Tauri stars associated with the MBM 12 complex (Magnani et al. 1995; Pound 1996), and the discovery of marginally bound dense cores (Reach et al. 1995) suggests that the cloud may form additional stars. There is also evidence for star formation in the southern hemisphere high-latitude cloud G316.5 + 21.0, a member of our sample. The cloud has a 100 μm *IRAS* intensity which is more than 20 times stronger than the average intensity of the Table 1 HLC

sample, which suggests that this cloud may be heated internally. Since the *IRAS* and CO maps for this source possess similar morphologies and since the *IRAS* peak coincides with the peaks of the CO and [C I] emission, we assume that the *IRAS* source is associated with the molecular cloud. Assuming the cloud is at a distance of 100 pc, its total *IRAS* luminosity is $2.5 L_{\odot}$. *IRAS* maps indicate that the source size is $\lesssim 100''$, and the colors for the associated *IRAS* point source ([25–12] = 0.06; [60–25] = 0.88; [100–60] = 0.48, where $[i - j] \equiv \log [I_i/I_j]$) are consistent with the source being an embedded star (cf., Emerson 1988). Future study of this source may provide clues as to the conditions necessary for star formation in translucent molecular clouds.

5. CONCLUSIONS

We have detected neutral atomic carbon [C I] emission toward all eight high-latitude molecular clouds which we have observed with the newly installed AST/RO telescope. The C/CO column density ratio in all 10 HLCs observed in [C I] to date ranges from 0.4 to 2.5 and averages ~ 1.2 . This confirms the photochemical model prediction that translucent clouds are the transitions between clouds with most of their carbon in C and clouds with most of their carbon in CO. *IRAS* observations of the 10 cloud sample imply total gas column densities of $N_{\text{H}} \approx (0.1\text{--}3.0) \times 10^{21} \text{ cm}^{-2}$. The C/CO ratio decreases with increasing N_{H} , also consistent with the predictions of photochemical models. Models of homogeneous clouds cannot be used quantitatively, however, unless we either invoke unreasonably high gas volume densities or make some assumptions regarding telescope beam filling. We conclude that more detailed models of the clouds, which take into account beam dilution of dense clumps, are necessary to interpret the data properly. One of the clouds in our sample, G316.5 + 21.0, contains a low-mass star. Further study of this source may help to constrain theories of star formation in pressure-bounded translucent regions.

Most of the molecular gas in the Galaxy is translucent, and our understanding of the photochemistry of translucent gas is incomplete without C I measurements. Until recently, the study of atomic carbon in the interstellar medium has been limited primarily to regions with high C I surface brightness and enhanced FUV fields. The AST/RO telescope has therefore opened a new window on the study of translucent gas in the interstellar medium.

We thank Alberto Bolatto for enlightening discussion and helpful suggestions. This research was supported in part by the National Science Foundation under a cooperative agreement with the Center for Astrophysical Research in Antarctica (CARA), grant number NSF DPP 89-20223. CARA is a National Science Foundation Science and Technology Center.

REFERENCES

- Anders, E., & Grevesse, N. 1989, *Geochim. Cosmochim. Acta*, 53, 197
 Boulanger, F., & Péroul, M. 1988, *ApJ*, 330, 964
 Chamberlin, R. A., Lane, A. P., & Stark, A. A. 1997, *ApJ*, in press
 Chiar, J. E., Kutner, M. L., Verter, F., & Leous, J. 1994, *ApJ*, 431, 658
 Emerson, J. P. 1988, in *Formation and Evolution of Low Mass Stars*, ed. A. K. Dupree & M. T. V. T. Lago (Boston: Kluwer), 193
 Engargiola, G., Zmuidzinas, J., & Lo, K.-Y. 1994, *Rev. Sci. Instr.*, 65, 1833
 Gir, B.-Y., Blitz, L., & Magnani, L. 1994, *ApJ*, 434, 162
 Habing, H. J. 1968, *Bull. Astron. Inst. Netherlands*, 19, 421
 Heithausen, A. 1996, *A&A*, 314, 251
 Hollenbach, D. J., Takahashi, T., & Tielens, A. G. G. M. 1991, *ApJ*, 377, 192
 Ingalls, J. G., Bania, T. M., & Jackson, J. M. 1994, *ApJ*, 431, L139 (IBJ)
 ———. 1997, in preparation
 Keto, E. R., & Myers, P. C. 1986, *ApJ*, 304, 466
 Langer, W. D., & Penzias, A. A. 1993, *ApJ*, 408, 539
 Low, F. J., et al. 1984, *ApJ*, 278, L19
 Magnani, L., Caillault, J.-P., Buchalter, A., & Beichman, C. A. 1995, *ApJS*, 96, 159
 Magnani, L., Hartmann, D., & Speck, B. G. 1996 *ApJS*, 106, 447

- Minh, Y. C., Park, Y.-S., Kim, K.-T., Irvine, W. M., Brewer, M. K., & Turner, B. E. 1996, *ApJ*, 467, 717
- Polk, K. S., Knapp, G. R., Stark, A. A., & Wilson, R. W. 1988, *ApJ*, 332, 432
- Pound, M. W. 1996, *ApJ*, 457, L35
- Pound, M. W., Bania, T. M., & Wilson, R. W. 1990, *ApJ*, 351, 165
- Reach, W. T., Pound, M. W., Wilner, D. J., & Lee, Y. 1995, *ApJ*, 441, 224
- Schieder, R., Tolls, V., & Winnewisser, G. 1989, *Exp. Astron.*, 1, 101
- Snowden, S. L., McCammon, D., & Verter, F. 1993, *ApJ*, 409, L21
- Spaans, M. 1996, *A&A*, 307, 271
- Stark, A. A., et al. 1994, *Antarctic J. US*, 29, 344
- . 1997a, in preparation
- Stark, A. A., Chamberlin, R. A., Ingalls, J. G., Cheng, J., & Wright, G. 1997b, *Rev. Sci. Inst.*, in press
- Stark, R. 1995, *A&A*, 301, 873
- Stark, R., & van Dishoeck, E. F. 1994, *A&A*, 286, L43
- Tielens, A. G. G. M., & Hollenbach, D. 1985, *ApJ*, 291, 722
- Turner, B. E. 1993, *ApJ*, 405, 229
- van Dishoeck, E. F., & Black, J. H. 1988, *ApJ*, 334, 771
- van Dishoeck, E. F., Black, J. H., Phillips, T. G., & Gredel, R. 1991, *ApJ*, 366, 141
- Zmuidzinas, J., & LeDuc, H. G. 1993, *IEEE Trans. Microwave Theor. & Tech.*, 40, 1797